Solar hydrogen from North Africa to Europe through greenstream: A simulation-based analysis of blending scenarios and production plant sizing

Solar Hydrogen from North Africa to Europe through Greenstream: a simulation-based analysis of blending scenarios and production plant sizing

Marco Cavana, Pierluigi Leone*

Dipartimento Energia "Galileo Ferraris", Politecnico di Torino

Corso Duca degli Abruzzi 24, 10129 Torino, Italy

*Corresponding author: Pierluigi Leone (pierluigi.leone@polito.it)

Abstract

Green hydrogen has recently gained a huge interest as a fundamental energy carrier to achieve Europe's climate neutrality by 2050. The European Commission sets clear political commitment to create a coordinated and financially supported roadmap for an infrastructural uptake of hydrogen. In this context, the hydrogen blending within the existing gas infrastructure is seen as a first move in the direction of the decarbonization of the gas sector and towards power and gas sector integration.

This paper aims at the transient and multi-component fluid-dynamic model of a gas transmission network with hydrogen and natural blends of one important North Africa-European gas corridor, the Greenstream connecting Libya to Italy. Starting from the available data on the gas imports at the Italian gas terminal, the operation of the whole infrastructure (up to the Wafa production plant in the Sahara Desert) has been simulated on the basis of the information and the assumptions on the gas compression station under increasing hydrogen blending scenarios (from 0 to 20%, with 5% steps).

The additional cost in terms of additional compression energy required, as well as the number of compressors' operating hours have been evaluated under the hypothesis that the energy content of the transported gas is maintained.

Additionally, the assumption of constant-in-time hydrogen volumetric shares resulted in a mismatch with the possible hydrogen production profiles from dedicated photovoltaic plants. The last part of this work is devoted to size the photovoltaic plants so to minimize the need for compressed hydrogen storage.

While the additional energy costs of transporting hydrogen blends are up to 32.5 % higher than natural gas transport, the mismatch between hydrogen production and the maximum receiving potential of the pipeline highlights a challenge to be tackled in order to boost intersectoral integration.

1 Introduction

The upcoming decade appears to be crucial for what concerns the efforts towards the energy transition and the achievement of long-term sustainability goals, especially for Europe. Even though the 2030 climate and energy framework was adopted in its final version in 2018, setting the collective target of cutting the greenhouse gas emissions at 40 % [1], the new European Green Deal [2] pushed the commitment forward. Consistently with these plans and thanks to the significant investment pulse from the Next Generation EU recovery plan [3], new strategy for energy system integration [4] and for hydrogen uptake [5] have been formally adopted. According to [6], hydrogen can play a major role in decarbonizing the energy system thanks to its versatility of use in transportation, electricity and heating provision, storage and grid services and as a commodity for industrial applications, provided that it is produced from low-emission sources. At present, all of the hydrogen produced (which is mainly used as feedstock) comes from fossil origin: 76% comes from steam reforming of natural gas and the rest from coal, thus producing 830 $MtCO_2/yr$ [7]. Usually, these CO_2 emissions are not captured thus this production pathway originates the so-called "grey hydrogen", which is the cheapest one. This already existent value chain of hydrogen may be transitioned towards sustainability by capturing and storing the carbon emissions thus originating the so-called "blue hydrogen". But when talking about the crucial role of hydrogen within the energy system, it is the "green hydrogen" that is mainly addressed, which is the one produced via electrolysis powered by electricity from renewables. A comparison in terms of greenhouse gas emission of the different hydrogen production alternatives is given in [8].

Hydrogen from renewables can thus have a prominent role not only for the decarbonization of fuel system (natural gas in particular) but also as a cross-sectorial link. As an energy vector, crucial is the opportunity that hydrogen offers to avoid the requirements for instantaneous supply-demand balancing thanks to the many possibilities to store it easily at large scale [9] with promising environmental outcomes if the electricity source would be renewable [10].

The role of hydrogen and other renewable gases (biomethane, syngas) for the long-term deep decarbonization of the energy system has been widely recognized in recent years. In a matter of two years, between 2018 and 2020, the role of renewable gases and hydrogen have changed from marginal [11] to the core of the gas industry strategy for the future [12]. European scenarios at 2050 show that their uptake may offer decarbonization options which are cheaper than deep electrification by between 94 [13] and 138 [14] billion € per year. Savings from choosing the deployment of hydrogen in 100% renewable cities are obtained also in [15]. The limits of the electrification are highlighted in [16] and [17]: starting from the current situation in which electricity use in final consuption is about 20%, scenarios at 2050 foresee an increase of its share up to, respectively, 29% (current policy) or 50% (in order to meet climate goals). According to IRENA, in order to achieve the Paris Agreement goals, the 8% of the global energy consumption should be provided by hydrogen at 2050 [18]. Interestingly, the renewable gases have been modeled in details for the first time in 2019 World Energy Outlook by IEA [19] which also dedicated an special insight on the role of gas infrastructure and its greenen for the energy transition. The IEA finds a very limited uptake of them under the "Stated Policy Scenario" where renewable gases will contribute only for the 1.6 % to the global gas demand

at 2040. On the contrary, the ”Sustainable Developement Scenarios” shows that this share could be as high as 6.5% in order to meet the climate goals.

The role of gas infrastructure appears to be fundamental in the evaluation of the economic advantage of investing in renewable gases. Avoinding a potential stranded asset by repurposing or retooling the european gas infrastructure can generates 217 billion € savings per year, according to [20]. However, the conversion towards renewable gases of the entire gas infrastructure would affect the whole natural gas value chain, especially if hydrogen will take the prominent role. There is in fact a wide consensus that the first phase for the hydrogen penetration into the gas market will be both through the creation of the so called ”Hydrogen Valleys” and the hydrogen blending within the gas infrastructure.

A number of previous studies have reviewed the readiness of the gas system towards the presence of hydrogen blendend within the natural gas. An extensive review of the opportunities and the criticalities of hydrogen admixture within the current gas infrastructure is given in [21]. In [22] maximum values of admissible hydrogen concentrations are given for a number of different areas of the overall gas system concluding that no major issues should be met up to concentration of 15% - 20%. However, in presence of Compressed Natural Gas (CNG) fuelling station or gas turbines the limit may need to be 1% or lower due to the current standards for veichle tanks. What is more, undergound storage system other than salt caverns requires further investigation. A comprehensive overview of the available test results have been presented by Marcogaz in [23]. Some limitations may derive from materials limits [24] or from the high sensitivity towards gas quality. This stands especially for turbines, gas burners and boilers for which the variation of gas quality may affect the stability of the combustion with potentially detrimental consequences in terms of the increase of pollutant emissions [25] and safety risks [26]. Even though these results calls for the need of more experiental trials and the definition of new hydrogen blends oriented testing methodologies, results from Siemens [27] and more rcently form Baker-Huges [28] show no major issue emerged in powering gas turbines and turbocompressors with 10% hydrogen blends. However, in order for the hydrogen economy to uptake by means of the hydrogen blending, it is urgent that the natural gas quality standards at european level will be harmonized as soon as possible. In this sense, the European Commission delegated the mandate M/400 EN [29] to the European Committee for Standardization (CEN). The publication of the norm EN 16726:2019 [30] on standardisation of gas quality (group H) was an outcome of it. Here the case of hydrogen injection is mentioned in an informative annex, reporting the results already presented in [22] and concluding with the impossibility of setting a common limiting value for hydrogen in the European infrastructure and recommending a case by case analysis.

The need for a significant pulse from decision makers towards a hydrogen economy is thus clear given the vast implication on gas sector and end users. The hydrogen strategy for a climate-neutral Europe [5] is specifically devoted to the definition of a precise roadmap towards 2030 and 2050 for a creation of a complete hydrogen ecosystem. By means of the creation of the Clean Hydrogen Alliance, the EU intends to put in practice a strategic roadmap consisting in the realization of large-scale projects and the creation of a suitable investment agenda. At present, the first phase foresees the realization of at least 6 GW of electrolyzers in the

EU by 2024, mostly devoted to the decarbonization of the already existing hydrogen production. A second phase to 2030, known as "the 2x40 GW" initiative, sets the goal of installing at least 40 GW of electrolyzers within Europe and additional 40 GW of electrolyzers capacity in North-Africa and Ukraine [31]. Along with these policy statements, a report by several European natural gas TSOs aimed at providing the first proposal of a roadmap to a fully developed continental hydrogen infrastructure [32]. While the goal is to build up a 100% hydrogen infrastructure by late 2040s – 2050, the hydrogen blending is considered an earlier option (already for the 2020s) to deploy hydrogen in the pipeline. While in [32] the focus is on the infrastructure and on the domestic production, in report [33] the possibility to produce green hydrogen from the solar and wind resource of North Africa is considered. This area is both rich in renewable resources and connected through natural gas pipelines to southern Europe as highlighted in [34].

In this context, this paper aims to simulate the transport of hydrogen from North Africa to Europe through the existing gas transport infrastructure, setting its focus in particular on the Greenstream, connecting southern Italy to Libya. The hydrogen is assumed to be mixed with the extracted natural gas so that it is transported as a blend. Differently from [35], the fluid-dynamic model of the gas network is a transient one. Previous works on the modelling of hydrogen blending in which transient model of the gas networks are used are [36] and [37]. In [36] the hydrogen injection is performed along a pipeline and follows a given pattern, so to result in a H_2-NG blend with varying concentration; in [37], a detailed multi-component, thermal and fluid-dynamic model is applied to a pipeline in order to simulate the propagation of gas quality perturbations when hydrogen is injected. These works aimed at modelling the impact of hydrogen blending as a form of renewable energy storage within the gas pipelines. The only constraint that is considered is the hydrogen availability (depending on the renewable electricity excess). On the contrary, in this work, the constraints imposed by the natural gas infrastructure are considered first. The share of hydrogen blended within the natural gas is kept constant (as in [38]) in view of the importance that gas quality stability may have for the final appliances. The infrastructure is modelled by means of a fluid-dynamic gas network solver as described in [39], which includes a model for the gas compression stations. Unlike [39], the gas flowing within the pipelines is modelled by means of a more sophisticated equation of state (the GERG-2008 [40]) thus the whole model is sensitive to the different composition of the hydrogen-natural gas blends.

The fluid-dynamic simulations consist in four blending scenarios under increasing hydrogen fraction (5%, 10%, 15% and 20%) with the twofold goal of estimating the impact of the hydrogen presence on the gas transport and of evaluating the patterns of hydrogen acceptability. The impact on transport is quantified in terms of variation of the compression work at the compression stations. As for the hydrogen acceptability patterns, they are the outcome of the gas pipeline and gas compressor modelling which is based on the available data on natural gas imports at the gas terminal of Gela (Sicily, Italy). These patterns are then used, together with the solar irradiation curve, to evaluate the mismatch between hydrogen production from photovoltaic source and hydrogen acceptability by the gas infrastructure. Finally, a design is proposed for the photovoltaic fields based on the minimization of the hydrogen storage needs.

With respect to the existing literature (e.g. [34]), the novelty of this work lies on the modelling oriented approach aimed at determine the impact of hydrogen blends on the gas pipeline operations resulting in higher operation costs in terms of energy, a different duty cycle and the failure in maintaining the required pressure level in some extreme cases. What is more, the question of mismatch between pipeline availability to accept hydrogen and solar hydrogen production is addressed, assuming that the gas quality is to be maintained constant. This operational hypothesis (it is not a real physical constrain on infrastructure or final appliances) offers a new point of view for the evaluation of potential and challenges of the electricity-gas sectorial integration.

The paper is structured as follows: in the next section, Paragraph 2, a detailed description of the gas network model is given, focusing on the assumptions made on the compressor station equation and on its control strategies. The case study is presented in the Paragraph 3, where a description of the technical features of the Greenstream are given and four hydrogen injection scenarios are described. The results of the simulations are given in the Paragraph 4 where they are compared with the base case scenario (non-injection scenario). Based on the results of the hydrogen injection profiles and the solar profile, a design procedure is then set-up in order to size the photovoltaic plants needed for providing a constant share of hydrogen. The procedure aims at minimize the need for hydrogen storage which is assumed to be in pressurized form, this is shown in Paragraph 5. Finally, a discussion of the results leading to the conclusions are performed in Paragraph 6.

2 Methodology

In order to evaluate the impact that the different levels of hydrogen blending cause on the fluid-dynamic of the gas pipeline and, consequently, to the operations of the gas compressor, a fluid-dynamic model of the infrastructure, including the pipelines and the compression stations is used. The expected outcomes of the simulations are the pressure level and the gas flows throughout the whole infrastructure which result from the boundary conditions applied. In this case, the outlet gas flows (i.e. the gas required at users' side) are known thus the profile of the gas at the infrastructure inlet is calculated. These profiles depend also on the compression stations operations which, in turn, depend on the calculated pressure level at the end of the pipeline. The resulting operation cycle of the compressors is evaluated in terms of the compression energy required and the gas consumption profile, which will be different across the four blending cases, allowing the calculation of the number of operative hours, the total gas consumption and the transport efficiency. The resulting gas profiles at the gas infrastructure inlet allow calculating the corresponding hydrogen injection profile which is needed to form the hydrogen share in the corresponding blending case. This hydrogen pattern is compared to the nominal potential hydrogen production profile from a photovoltaic power plant to highlight possible mismatches between hydrogen production and the pipeline availability to accept it. A sizing procedure of the photovoltaic plants at the gas infrastructure inlet locations is proposed. The mismatch calls for the need of a certain storage capacity thus the sizing procedure is based on the minimization of the hydrogen storage capacity. It is assumed that hydrogen is stored in compressed form.

2.1 Pipeline model

The motion of a fluid within a pipeline is governed by a system of three partial differential equations (PDEs): the conservation of mass, momentum and energy. In case of iso-thermal fluid-flow simplification (as in the model here described), the system of PDEs is reduced to the mass and momentum equation as follows:

Conservation of Mass

$$\frac{\partial \rho}{\partial t} + \frac{\partial (\rho v)}{\partial x} = 0 \tag{1}$$

Conservation of Momentum

$$\frac{\partial (\rho v)}{\partial t} + \frac{\partial (\rho v^2)}{\partial x} + \frac{\partial p}{\partial x} + \frac{\lambda \rho v |v|}{2D} + \rho g sin\alpha = 0 \tag{2}$$

where ρ is density, v is velocity, p is pressure, λ is friction factor, D is the pipeline diameter, g the gravitational acceleration and α the pipeline inclination angle.

As the modelled network regards a compressible fluid, Eq. (1) cannot be further simplified while the second term of Eq. (2) (the convective term) can be neglected, as the maximum velocity of gas within pipelines does not exceed 10 ÷ 25 m /s.

The system of equation is characterized by two equations in three unknowns thus a closure equation is required, this being the Equation of State

$$\frac{p}{\rho} = c^2 = Z\,R\,T \tag{3}$$

where c is the isothermal speed of sound and $Z = Z(p, T, [y])$ is the compressibility factor, a function of pressure, temperature and gas composition $[y]$. The way the compressibility factor is determined defines which equation of state is chosen to solve the problem. In this case, the GERG-2008 equation of state [40] has been chosen, being one of the most recent developed, wide-range, multi-component equation of state. In fact, it is sensitive to the composition of the natural gas considered, being able to account for 21 different chemical species within the natural gas, including hydrogen.

In order to derive a proper pipeline equation, it is convenient to substitute the velocity v with the mass flow rate $\dot{m}$ by means of the following relation:

$$\dot{m} = \rho v A \tag{4}$$

In this way, the pipeline equation relates the main operational variables of a duct: pressure and gas flow. By substituting Eq. (3) and (4) in Eq. (2) and rearranging the terms, it is possible to obtain a differential expression of the pressure drops along a pipeline:

$$\frac{\partial p}{\partial x} = -\frac{1}{A}\frac{\partial \dot{m}}{\partial t} - \frac{\lambda c^2}{2DA^2 p}\dot{m}|\dot{m}| - \frac{g sin\alpha}{c^2}p \tag{5}$$

which results in a composition of several terms such as:

- inertia, related to the time derivative of the mass flow, accounting for the forces which oppose the flow acceleration direction;
- hydraulic resistance accounting for the friction which is quadratically proportional to the mass flow and it oppose the mass flow direction;
- gravitational resistance accounting for the pressure losses due to gravity if the pipeline has an inclination α.

In the form of Eq.(5), the pressure drops equation displays non-linearity both on mass flow and on pressure. Some further elaborations are required to get to a linearized form, which is suitable for network modelling purpose.

First, the non-linearity associated with the pressure can be avoided by performing a substitution of variable such as $P = p^2$, thus referring to the quadratic pressure, obtaining:

$$\frac{\partial P}{\partial x} + \frac{2g sin\alpha}{c^2}P = -\frac{2\,p}{A}\frac{\partial \dot{m}}{\partial t} - \frac{\lambda c^2}{DA^2}\dot{m}|\dot{m}| \tag{6}$$

The presence of the time and spatial derivatives requires the adoption of integration strategies. Regarding the integration of the spatial derivative, Eq. (6) can be considered as a linear and non-homogeneous differential equation of first order provided that the coefficients of the right-hand side are averaged over the pipe section $\Delta x = l$, so to be constant with respect to the x. Assuming this approximation, the equation is solved analytically yielding to the following pipeline equation:

$$P_{in} - P_{out}e^{s_j} = \frac{2\,\bar{p}_j\,l_{e_j}}{A_j}\frac{\partial \dot{m}_j}{\partial t} + \frac{\lambda_j\,\overline{c^2}_j\,l_{e_j}}{D_j A_j^2}\,\dot{m}_j|\dot{m}_j| \tag{7}$$

with:

$$l_{e_j} = \begin{cases} l_j\,, & h_{in} = h_{out} \\ \dfrac{e^{s_j}-1}{s_j}\,l_j\,, & h_{in} \neq h_{out} \end{cases} \qquad s_j = \frac{2g(h_{out} - h_{in})}{\overline{c^2}_j}$$

Where subscripts *in* and *out* stand for the inlet and the outlet sections of the generic j^{th} pipe. In order to account for the gravitational contribution, the "effective length" l_e is defined as the corrected length of the pipeline section in case of non-horizontal pipelines (whose slope is defined by the elevation difference $(h_{out} - h_{in})$ of their ends.

The averaged quantities, which make the analytical solution possible, are calculated starting from the computed value of the average pressure $\bar{p}$ as expressed in [41] and here reported:

$$\bar{p} = \frac{p_{in}^2 + p_{in}p_{out} + p_{out}^2}{p_{in} + p_{out}}$$

And in turn:

$$\overline{c^2} = Z(\bar{p}, T, [y])RT$$

Eq. (7) has now the form of an ordinary differential equation in which the time derivative can be treated by means of an implicit finite different scheme for the approximation of the inertia term, leading to the following expression:

$$P_{in}^{n+1} - P_{out}^{n+1} e^{s} = \frac{2\,\overline{p^{n+1}}\,l_e}{A\,\Delta t}(\dot{m}^{n+1} - \dot{m}^{n}) + \frac{\lambda\,\overline{c^2}\,l_e}{DA^2}\dot{m}^{n+1}|\dot{m}^{n+1}| \qquad (8)$$

This scheme is a single-step backward differentiation formula also known as backward Euler method. It is one of the most common and basic numerical method for the solution of ordinary differential equations with first-order convergence and fully implicit feature, so to guarantee stability for large timesteps, as reported in [42] and in [43].

The integrated form of the pipeline equation is finally given in a more concise form as follows

$$\Delta P^{\,n+1} = R_I \cdot (\dot{m}^{\,n+1} - \dot{m}^{\,n}) + R_F \cdot \dot{m}^{\,n+1}|\dot{m}^{\,n+1}| \qquad (9)$$

with ΔP representing the corrected and quadratic pressure drop as defined here

$$\Delta P^{\,n+1} = P_{in}^{n+1} - P_{out}^{n+1} e^{s}\,;$$

and the coefficients of the right-hand side grouped in two resistance coefficients

$$R_I = \frac{2\,\overline{p^{n+1}}\,l_e}{A\,\Delta t}\,; \qquad R_F = \frac{\lambda\,\overline{c^2}\,l_e}{DA^2} = \frac{16\,\lambda\,\overline{c^2}\,l_e}{\pi^2 D^5}\,;$$

The two terms in the right-hand side of the Eq. (9) represent the two physical phenomena contributing to the pressure variation along the pipeline: The inertia contribution (subscript I) and the fluid-dynamic friction (subscript F)

The quadratic pressure-drop equation as expressed in Eq. (9) is a parabolic function of the mass flow. In order to be included in an algorithm for the network simulation, it has to be linearized. Considering the generic pipe j and assuming the linearization point as $\left(\Delta P_j^{n+1}, \dot{m}_j^{n+1}\right)$, the application of the linearization formula leads to the following expression:

$$\Delta P_j^{n+1\,(k+1)} - \Delta P_j^{n+1\,(k)} = \left.\frac{d\Delta P_j^{n+1\,(k)}}{d\,\dot{m}_j^{n+1\,(k)}}\right|^{(k)} \left(\dot{m}_j^{n+1\,(k+1)} - \dot{m}_j^{n+1\,(k)}\right)$$

from which, solving the derivative of the pressure drop Eq. (9), it is possible to obtain the final expression:

$$\Delta P_j^{n+1\,(k+1)} - \left(2R_F \cdot \left|\dot{m}_j{}^{n+1\,(k)}\right| + R_I\right)\dot{m}_j{}^{n+1\,(k+1)} = \qquad (10)$$

$$= -\,R_F \cdot \left|\dot{m}_j{}^{n+1\,(k)}\right| \dot{m}_j{}^{n+1\,(k)} - R_I \dot{m}_j{}^{n\,(k)}$$

This method was presented in [44] for the steady state case and generalized for the application to the transient equation in [39].

In the end, in order to refer to the normal pressure drop Δp rather than the corrected-square pressure drop ΔP, the Eq. (9) and its linearized version (10) which are generally applied to the pipeline j, shall be divided by $(p_{in} + p_{out} e^{s/2})$.

2.2 Compression Station Model

Within the gas network infrastructure, the compressor stations are active, non-pipeline elements that are fundamental to guarantee the gas transport along the pipelines. They usually consist in a number of centrifugal compressors, powered by gas turbines, which consume a fraction of the natural gas from the grid. The compression units may be in a series or parallel configuration. Usually series (or multistage) configurations allow higher compression ratios, while parallel ones allow higher flow rates. Additionally, a gas compression station is equipped with gas coolers in order to cool down the gas which has heated up after the compression far higher than the acceptable pipeline temperature.

In this modelling framework, the compression station is considered as a black box which contains the combination of all the installed compressors and the gas coolers. In this way, the outlet gas temperature can be assumed as the same as the one assumed throughout the system. The general form of the gas compressor equation, referred to the mechanical shaft power ($P_{mech_{shaft}}$) required by the compressor to the gas turbine driver, results in:

$$P_{mech_{shaft}} = \frac{1}{\eta_{is}\,\eta_{mecc}} \frac{\gamma}{\gamma - 1} Z_{in} T_{in} R_{in} \left(\beta^{\frac{\gamma-1}{\gamma}} - 1 \right) \dot{m}_j \qquad (11)$$

with η_{is} the isentropic efficiency of compression, η_{mecc} the mechanical efficiency of the compressor (set equal to 80%), γ the adiabatic exponent and β the compression ratio which is the ratio between outlet and inlet pressure.

The fuel offtake required to power the whole gas compression station may be derived as follows:

$$\dot{m}_{consumption} = \frac{P_{mech_{shaft}}}{\eta_{turb}\, HHV} \qquad (12)$$

with η_{turb} the turbine efficiency (which includes the expansion efficiency and the combustion efficiency) and HHV the higher heating value of the natural gas (or H_2-NG blends).

Typical ranges for η_{is} , η_{turb} and β are given in the following table:

Table 1 – Typical ranges for isentropic efficiency, mechanical drive efficiency and compression ratio for a gas network compressors [45], [41]

η_{is} [%]	η_{turb} [%]	β [-]
75 ÷ 84	28 ÷ 38	< 2

In order for the compressor equation to be integrated within the complete linear set of equation of the gas infrastructure model, a linearized version of the compressor equation is obtained as Eq. (13). In this form, the amount of the extracted fuel from the network to power the turbo compressor is also accounted and it is assigned to the gas compressor inlet node. In this way it is possible to calculate the amount of gas consumed by the compressor itself.

$$-\frac{K_i \dot{m}_j}{p_i}\beta^{\frac{\gamma-1}{\gamma}} \cdot p_i + \frac{K_i \dot{m}_j}{p_o}\beta^{\frac{\gamma-1}{\gamma}} \cdot p_o + \frac{K_i\,\gamma}{\gamma-1}\left(\beta^{\frac{\gamma-1}{\gamma}}-1\right)\cdot \dot{m}_j + \dot{m}_{consumption} = 0 \quad (13)$$

with:

$$K_i = \varphi \frac{Z_i T_i R}{\eta_{ad}\,\eta_{mecc}\,\eta_{turb}\,HHV} ;$$

Where K_i is the fraction of the total installed power of the compression station.

The compressor may assume a number of different operational modes, depending on the choice of the control variable. In this work two possible control modes are considered: the compressor working at assigned β and the compressor controlled by the assigned shaft power. The compressor will work at assigned compression ratio when a minimum β is to be guaranteed or to comply with the limit of β_{max}. Otherwise, the compressor is controlled by the assigned shaft power. The compression station can either be by-passed or shut-down. In case of by-pass, the inlet and outlet pressure will be required to be equal. In case of shut-downs, the mass flow rate within the compressor will be set to zero. More details and assumptions on the operation of the gas compression station in this study are given in the "Assumptions and Simplifications" section.

2.3 Algebraic model of the gas infrastructure

In order to have a complete algebraic model of the gas infrastructure, the mass conservation equation has to be applied to each node of the network (i.e. joints between two pipeline sections). Having defined a control volume around each node, the integral form of the continuity equation may be obtained as follows:

$$\frac{V_i}{c^2}\frac{dp_i}{dt} = -\sum_j a_{i,j}\,\dot{m}_j - \dot{m}_{ext_i} \quad (14)$$

with:

$$V_i = \frac{\pi}{8}\sum_j D_j^2\,\Delta x_j ;$$

that is the geometrical volume of the i[th] node.

Introducing the concept of incidence matrix defined as follows:

$$\mathbf{A} = \left[a_{i,j}\right]^{n\times b}, \qquad a_{i,j} = \begin{cases} +1, & \text{node } i \text{ is the inlet of edge } j \\ -1, & \text{node } i \text{ is the outlet of edge } j \\ 0, & \text{node } i \text{ and edge } j \text{ have no connections} \end{cases} \quad (15)$$

where *n* is the number of nodes (connection between pipes) and *b* is the number of edges (pipes or other non-pipe elements such as compression station) as a way to express any network topology in matrix form, it is possible to express Eq (10) , Eq (13) and Eq (14) in matrix form as follows:

$$\mathbf{A_g^t}\, \boldsymbol{P}^{n+1\,(k+1)} - \mathbf{R}\, \dot{\boldsymbol{m}}^{n+1\,(k+1)} = -\mathbf{R_F}\left(\left|\, \dot{\boldsymbol{m}}^{n+1\,(k)}\right| \circ \dot{\boldsymbol{m}}^{n+1\,(k)}\right) - \mathbf{R_I}\, \dot{\boldsymbol{m}}^{n\,(k)} \tag{16}$$

$$\mathbf{C_{NP\,P}}\, \boldsymbol{p}^{n+1} + \mathbf{C_{NP\,M}}\, \dot{\boldsymbol{m}}^{n+1} + \mathbf{C_{NP}}\, \dot{\boldsymbol{m}}_{\boldsymbol{ext}}{}^{n+1} = \mathbf{0} \tag{17}$$

$$\boldsymbol{\Phi p}^{n+1} + \mathbf{A}\, \dot{\boldsymbol{m}}^{n+1} + \mathbf{I}\, \dot{\boldsymbol{m}}_{\boldsymbol{ext}}{}^{n+1} = \boldsymbol{\Phi p}^{n} \tag{18}$$

This set of equations are to be solved simultaneously for each time step of the simulation period, provided that suitable boundary conditions at the gas pipeline inlet and outlet are assigned. Because of the linearization of the pipeline equation, for each timestep the fluid-dynamic problem will be solved iteratively until the residue of the pipeline equation will be smaller than a given tolerance (usually 10^{-4}).

3 Case study description

3.1 Technical description of the Greenstream and the West Libyan gas infrastructure.

The European natural gas market heavily relies on imports. According to Eurostat [46], between 2017 and 2018 the share of annual imported natural gas grew form 74.4 % to 77.9 %, with Russian gas playing the prominent role, accounting for about 47 % of the imports, followed by Norway (about 30 %) and North-Africa (around 12 %). The latter region is connected to Southern Europe by means of four corridors, commissioned between 1983 and 2010 with an overall capacity of 61.2 bcm/y of natural gas. About the 67 % of this capacity is connected to the European system by means of the Italian natural gas transmission system, which is reached by the Trans-Mediterranean Pipeline (Transmed) and the Greenstream Pipeline in Sicily. This work will focus on the Greenstream corridor.

The Greenstream pipeline is the corridor carrying Libyan gas to the European market. It starts from the Libyan coast at Mellitah Complex where the gas compression station is located and it landfalls at Gela gas receiving terminal (Sicily, IT). It ends at Enna gas compression station where it connects to the Transmed route. Greenstream is the longest and the deeper submarine gasduct of the Mediterranean Sea, running about 520 km subsea and reaching a maximum depth of about 1150 m [47]. It is composed of a single pipe with a nominal diameter of 32 inches. The onshore section in Sicily is 67.3 km long [48].

Greenstream is a part of the Western Libyan Gas Project (WLGP), a joint venture between the Italian Eni and the Libyan National Oil Corporation (NOC), which had the goal of developing the oil and gas sector in Western Libya. The project had covered the development of two main extraction areas, the gas hub of Mellitah

and the entire connecting infrastructure along with the Greenstream. Today, Western Libyan natural gas is extracted from the Wafa oil and gas field, located onshore in the Sahara Desert near to the Tunisian border, about 520 km south-west far from Mellitah and the Bahr Es Salam offshore field, located 110 km far from the Libyan coast. Extracted oil and gas are both sent to the Mellitah Gas Processing plant where treatment facilities are located as well as the gas compression station of Greenstream and the local market gas reduction station.

Table 2 – Main technical features of the gas pipelines infrastructure of Western Libyan Project (in which Greenstream gas corridor is included)

	Segment				Length	# Pipes × Diameter	DN
	From	To			[km]		[mm]
	Wafa Field	Mellitah Hub	Libya	Onshore	520	1 × 32”	800
	Bahr Es Salam field	Mellitah Hub	Libya	Offshore	110	1 × 24”	600
Greenstream	Mellitah Hub	Gela Receiving Terminal	Sicilian Channel	Offshore	520	1 × 32”	800
Greenstream	Gela Receiving Terminal	Enna compression station	Italy	Onshore	67.3	1 × 36”	900

As it can be noted, the Mellitah Hub is a crucial point of both the Greenstream and the Western Libya oil and gas infrastructure. As for the natural gas sector, it receives the sales-ready natural gas from the Wafa field and the raw natural gas extracted from the offshore Bahr Es Salam field, coming from the Sabrata Platform. This stream of gas is treated at Mellitah Gas Treatment Plant and then it is integrated to the natural gas transmission system. The total amount of gas collected at Mellitah Complex is allocated between the export and the domestic market by means of the gas compression station and the gas reduction and metering station that are both located at the Mellitah Complex. The Mellitah Gas Compression Station is composed of 5 turbo-compressor trains. For each of the train, the gas turbine drives 2 barrel type centrifugal compressor in a tandem configuration through a speed increasing gear box [49]. The gas turbines are of the type MS5002D-DLN, with a rated power of 32.58 MW and an overall efficiency $\eta_{turb} = 29.4\%$ [50]. The turbo compressor total installed power of the site is 160 MW. The gas station is devoted to compress the gas for export purposes, up to a maximum operating pressure of 212 bar. At present, the annual maximum transmission capacity of the Greenstream pipeline is 11 billion Sm^3, which corresponds to about 30 MSm^3/d on average. The Mellitah gas reduction and metering station is instead designed to deliver up to 15 MSm^3/d for the domestic consumption by means of the 44 bar coastal line, operated by the Sirte Oil Company (S.O.C.) [47].

As for the production fields, the production capacity of the Wafa field is up to 2.8 MSm^3/d after the installation of four new gas compressors [51] and the production capacity of Bahr Es Salam field is up to 28.2 MSm^3/d [52].

3.2 Blending scenarios

Four blending scenario have been considered, ranging from 5% of hydrogen within natural gas on volume basis, up to 20%, with an increment of 5% for each scenario. Each blending case study is compared with the base case scenario consisting in a simulation of the current gas system operation. Given that the increase of the hydrogen molar fraction causes a decrease of the calorific value of the natural gas-hydrogen admixture, the simulations have been conducted considering the same amount of energy flow carried along the pipeline as the energy transported in the reference case of 0% hydrogen. This implies an increase of the volume flow rate of the natural gas and hydrogen blends. Under this assumptions, the hydrogen share is meant to substitute a portion of the fossil gas. Concerning the modelling strategy, the constraints on the outlet gas flow will be given in terms of chemical energy released.

The hydrogen-natural gas mixture has been assumed to be formed upstream the modelled gas infrastructure, at the two inlets of the network: Wafa Field and Mellitah hub. As the admixture process is out of the modelling domain, the gas quality throughout the infrastructure is then homogeneous throughout all the infrastructure and constant during the whole considered time interval for each scenario. The natural gas quality for the base case scenario is set equal to the composition of the Libyan gas for the thermal year 2017-2018 as specified by Snam at [53] and reported in Table 3. The composition will be re-proportioned accordingly as the hydrogen is mixed to the natural gas.

Table 3 – Typical natural gas composition and gas quality parameter for the Libyan gas for the thermal year 17-18 [53].

Chemical species		Libyan Gas [% mol/mol]
Methane		85.306
Ethane		6.486
Propane		2.058
Iso Butane		0.280
Normal Butane		0.437
Iso Pentane		0.099
Normal Pentane		0.063
Hexane +		0.015
Nitrogen		3.882
Carbon Dioxide		1.268
Helium		0.106
Oxigen		-
Gas quality parameter	**units**	
Higher Heating Value	[MJ/Sm^3]	39.586
Wobbe Index	[MJ/Sm^3]	49.158

Relative Density	[-]	0.64840

4 Assumptions and simplifications

4.1 Gas production and delivery

According to the data on the natural gas imports available on the transparency platform of ENTSOG [54], the annual import of natural gas from Libya to Italy varied between 4 and 6.5 billion Sm^3 during the years 2013-2019. These data show that the infrastructure is currently running at the half of its capacity. Figure 1 shows the average gas flow rates together with the standard deviation for each year. Even though the variations may be as high as 25%, the cumulative curves in Figure 1.b show that the imports are not affected by a summer/winter seasonality as the rate of increase is more or less constant throughout the year. This observed behaviour justifies the choice of the simulation time interval, corresponding to 10 days between November 7th and November 17th.

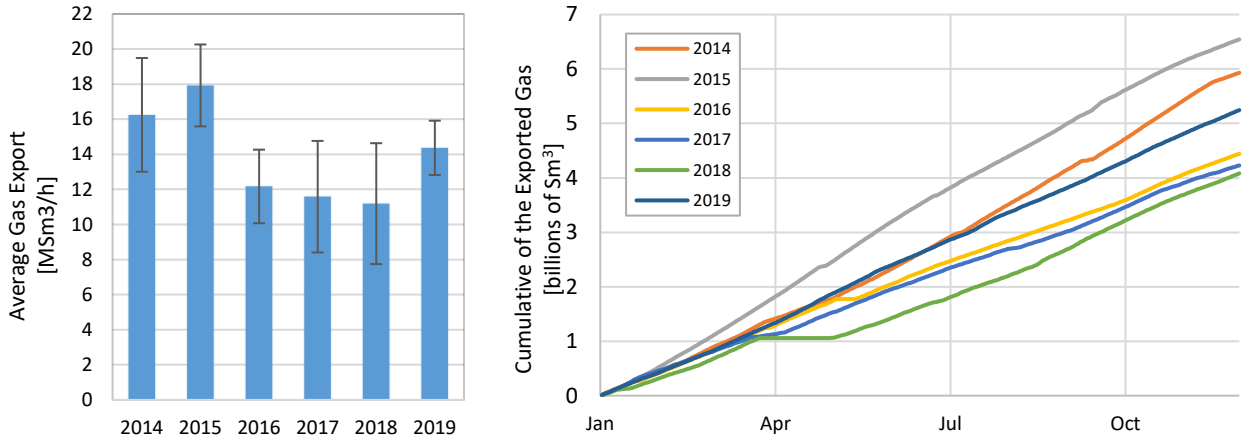

Figure 1 – Left: average daily gas export trough Greenstream. Right: cumulative of the daily gas export through Greenstream.

The gas export data towards Italy is the only set of data of the Western Libya infrastructure that are available with a daily or hourly time resolution. No detailed information about production rate at the production fields or about the amount of gas delivered to the domestic market are available. Thus, the following assumptions have been made based on the information about the capacities of the production or delivery points cited in the previous paragraph. As for the delivery to the internal Libyan market, the gas exiting the Mellitah hub towards the coastal line has been assumed to be equal to the half of the gas sent to the export. Regarding the production field, the Wafa one has a throughput capacity of 1/11 of the one of Bahr Es Salam. Thus, for

the sake of the simulations, it has been assumed that the allocation of the overall gas flow rate among the two fields will constantly follow these proportions.

4.2 Infrastructure

In order to model the effect of increasing molar fraction of hydrogen within the Libyan gas system, the western Libyan gas infrastructure has been simplified as reported in Figure 2.

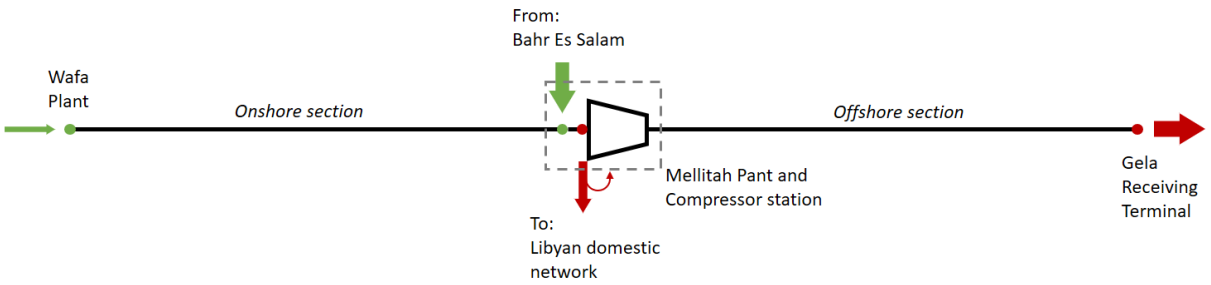

Figure 2 – Schematic of the modeled portion of Western Libya gas infrastructure including the onshore section from Wafa to Mellitah, the Mellitah plant and compression station and the submarine section of Greenstream until the Italian coasts.

The modelled infrastructure corresponds to a series of two pipelines connected by the Mellitah gas hub where the natural gas from the offshore platform of Bahr Es Salam is added to the stream from Wafa and a portion of the natural gas is delivered to the local market. Thus, the 110 km long pipeline between the offshore platform and the Mellitah Gas Processing Plant has been excluded from the study because it carries sour gas that is treated at the Mellitah plant. The treated gas resulting from the plant is integrated to the modelling framework considering an injection node at the end of the first section of the pipeline system. Similarly, the coastline domestic infrastructure is not modelled thus, for the sake of the simulations, a withdrawal node is considered upstream the gas compressor in which both the assumed amount of gas delivered to the local market and the gas consumption of the compressor are withdrawn.

The two pipes in series are both 520 km long with a nominal diameter equal to 800 mm. The first section is the onshore ducts running from Wafa Plant to Mellitah while the second section is the Greenstream offshore section from Mellitah Compessor station to the Receiving Terminal at Gela in Sicily. Both sections have been discretized with a 10 km long mesh. In Table 4 the technical details of the two pipeline sections are given.

Table 4 – Technical features of the modeled portion of the Wester Libyan Infrastructure (wall thickness data from [55]).

Segment			Length [km]	# Pipes × Diameter	DN [mm]	Outer diameter [mm]	Wall thickness [mm]	Inner diameter [mm]	Roughness [μm]
Wafa Field – Mellitah Hub	Libya	Onshore	520	1 × 32”	800	812.8	30.2	752.4	14

Greenstream	Mellitah Hub – Gela Receiving Terminal	Sicilian Channel	Offshore	520	1 × 32”	800	812.8	30.2	752.4	14

Given that the Greenstream is known to be the Mediterranean gas duct that reaches the deepest seafloor, the elevation of the entire path of the pipelines have been considered so to account for the gravitational terms of the momentum equation. The elevation profile have been obtained from [56] for what concerns the offshore section and reconstructing the pipeline path on Google Earth for the onshore section. In Figure 3 the overall profile is given.

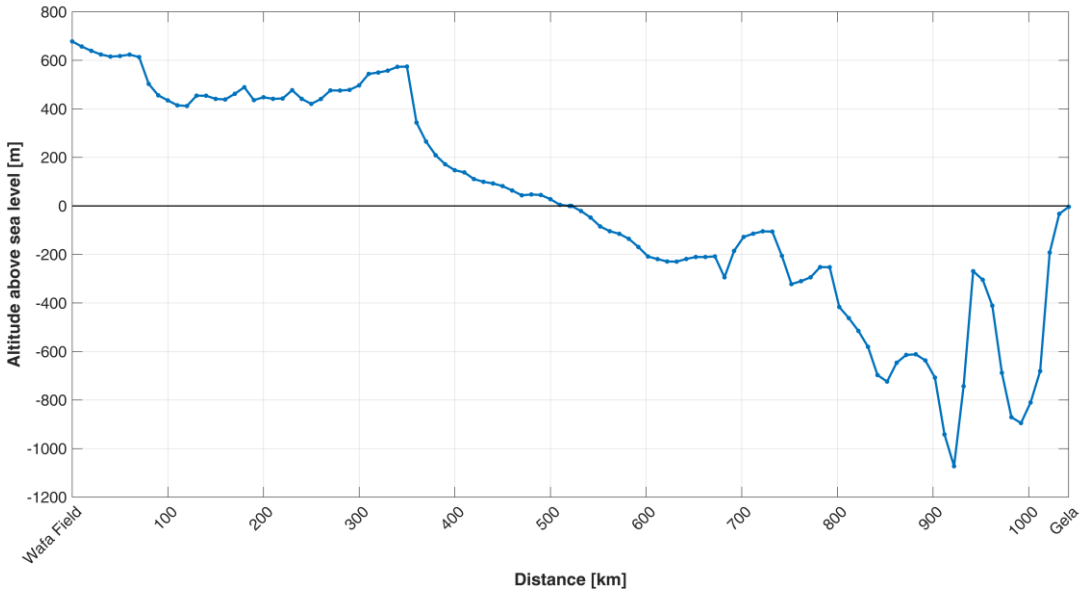

Figure 3 – Elevation profile of the modelled infrastructure.

4.3 Assumptions on the compressor station and its control strategy

According to [41], the typical compression ratio for a centrifugal compressor is lower than 2. Thus, it is assumed that the compression ratio range for the compressor in this model is $\beta = [1.2 – 1.8]$. The Mellitah Gas Compression station is assumed to have all the 5 turbo-compressors in parallel so that higher amount of flow rates may be elaborated while keeping the compression ratio within the range.

Concerning the compressor control strategy, each time the gas pressure at the inlet node is higher than the outlet node pressure, the compressor is by-passed and the entire infrastructure is operated under free-flow condition. Conversely, whenever the outlet pressure is higher than the inlet one, the “off mode” is applied so than no flow rate is passing through the compressor’s branch. The compressor is turned-on depending on the resulting pressure at the end of the Greenstrem pipeline, at the Gela Gas Receiving Station. In fact, according to [57], the minimum contractual pressure at the Gela entry point must be 70 bar_g. In order to comply with this contractual requirement, it was assumed that whenever the pressure at Gela drops below 95 bar_g, the

compressor station is turned on. Depending on the value of the pressure ratio between the outlet and the inlet nodes of the compressor, the compression station may be operated in two alternative modes:

1) Compression ratio controlled: if the ratio between outlet and inlet pressure is less than $\beta_{min} = 1.2$, the value of $\beta_{min} = 1.2$ is imposed as a constraint on the compressor equation;
2) Shaft Power assigned: if the compression ratio β is within the range, the shaft power is imposed as a constraint on the compressor equation.

When the compression station is operated according to the shaft power, the range of variation of the assigned power is Pshaft = [0 – 128] MW, following the redundancy principle mentioned in [57], for which a stand-by compressor having a rated power higher or equal to the rated power of each single active units is to be guaranteed. A compressor start-up rate has also been considered: a linear ramp of 6.5 MW every 10 min has been assumed, which is coherent with other compressor operation modes in gas transmission systems. The assigned shaft power increase continues as long as a drop of the gas pressure at the Gela receiving station is observed provided that the compression ratio β is within the ranges. Whenever the compression ratio exceeds $\beta_{max} = 1.8$, the gas station control mode changes again to the case of assigned compression ratio, which will be set equal to β_{max}.

5 Simulations and results

A time interval of 264 hours (11 days from gas day November 7th to gas day November 18th) has been considered to run the following simulations, with a time discretization of 600 s. The two 520 km long pipeline sections have been spatially discretized in 52 subsections of 10 km each. For what concerns the boundary conditions of the pipeline system, the real profile of gas export towards Italy have been applied to the Gela Receiving Terminal while the same profile but halved in magnitude have been applied to the gas outlet towards domestic market. To be noted that data from [54] are available with an hourly time resolution. In order to lower it at 10 minutes (600 s), a linear interpolation procedure was been applied. The gas flow boundary condition at Gela gas receiving station is given in Figure 4.

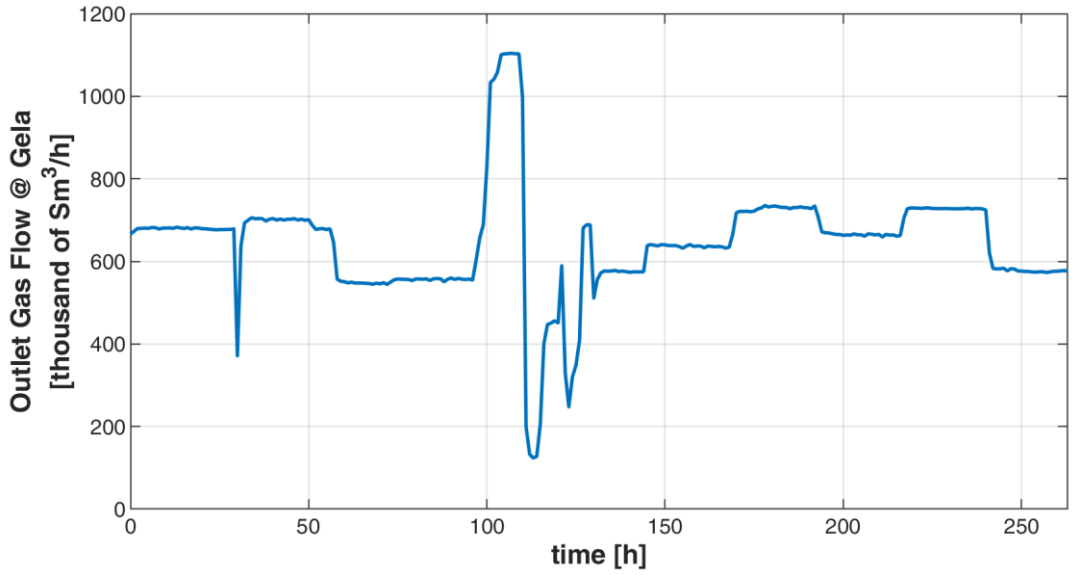

Figure 4 – Outlet gas flow rate set at Gela gas receiving station as a boundary condition Data for the period Nov.7th – Nov.17th 2017 from [54].

As for the gas inlet points, the Wafa field is assumed to be a pressure-controlled node (as it is a gas well output) set to a constant value of 75 bar_g, while for the gas inlet from the offshore fields, the condition on the gas flow allocation described in the previous section is assigned.

For each of the following simulations, a steady-state initial condition of the gas network is assumed, with the outlet pressure of the compression station set to 110 bar_g.

The alteration of the gas quality of the transported gas is expected to affect the gas fluxes and the operations of the gas compression station. The objective of the simulations is to quantify these effects.

5.1 Fluid-dynamic impacts of hydrogen blending

If the amount of chemical energy delivered at the outlet is kept constant, the amount of gas flow increases because the volume-based heating value of the blend decreases as the hydrogen molar fraction increases.

The blue line in Figure 5 shows the relation between the volume increment rates with respect to the increase of the hydrogen amount in the natural gas blend, under the hypothesis of supplying the same amount of energy. When 10% hydrogen is present within the natural gas, the gas volumetric flow is increased by 7.5% while at 20% of hydrogen, the gas volumetric flow is increased of 16.2 %. The relation is slightly less than linear (the dashed line marks the linear relation). The orange line represents the relation between the hydrogen molar fraction and its contribution to the energy content of the gas flow. It is worth to note that the 20% of the hydrogen fraction substitutes only the 7% of the energy content of the initial 100% fossil natural gas flow.

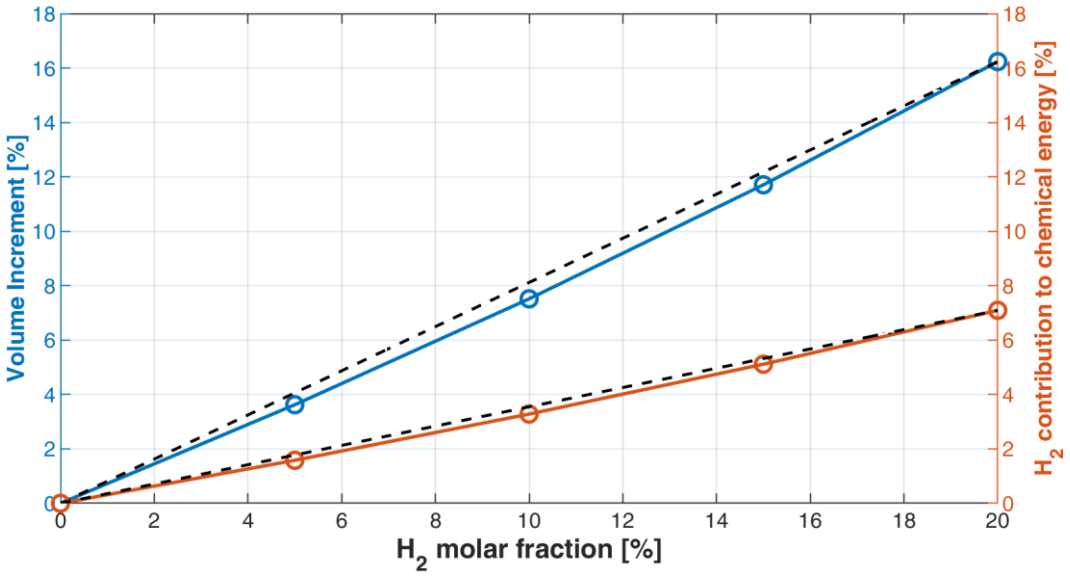

Figure 5 – Relation between the hydrogen molar fraction within the natural gas blend, the volume increment of the gas flow and the hydrogen energy contribution to the gas flow, under the hypothesis of constant energy output at the outlet nodes of the network.

The increase of the volume gas flow rate is the main cause of the increment of the pressure drop along the pipeline system. This results in a lower pressure at the outlet nodes. In Figure 6, the pressure profile at Gela gas receiving terminal is given for the whole simulation interval and for the five hydrogen blending cases. It is possible to see that the higher is the hydrogen fraction, the lower is the outlet pressure. At the initial time, the outlet pressure variation is as high as –15% for the case of 20% hydrogen. It gets to –17.9% at time t = 109 h when the lowest pressure value can be observed (corresponding to the maximum withdrawal interval). It is worth noting that the outlet pressures of all the cases with hydrogen injection drops below the minimum contractual pressure that should be guaranteed at Gela receiving station (i.e. p = 70 bar_g). This implies that a change in the compressors' control strategy would be required.

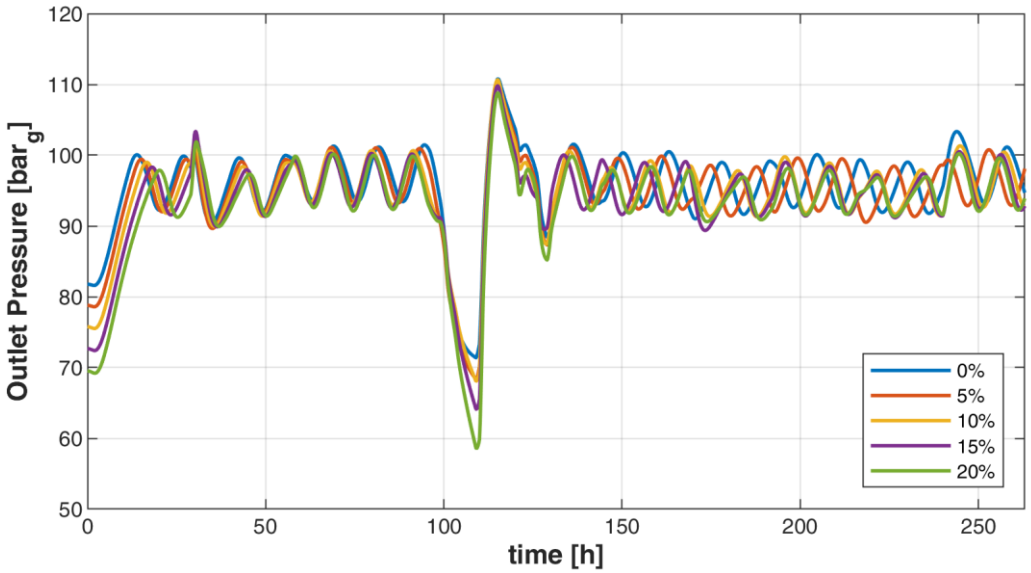

Figure 6 – Pressure profiles at the Gela gas receiving station under different molar fraction of hydrogen.

The second part of Figure 67 (for times higher than 120-150 h) shows the different pressure profiles going out of phase with respect to each other. This is a consequence of the variation in the gas station operation, as it will be clearer form the next figures.

Figure 7 shows both the number of hours in which the gas compression station is active and the compressors utilization factor, calculated as the ratio between the operating hours and the overall simulation hours. It is possible to see that as the hydrogen molar fraction increases, the number of operating hours of the compressor increases too, under the assumption that the compressor control strategy is maintained unvaried for all the five simulation cases. The results mean that in order to reach the outlet pressure set point the compressor needs to work longer. More specifically, the increment in the overall operating time interval with respect to the previous simulation scenario is between 9.5 and 12.3 hours. As it has been already commented for Figure 6, the longer operating time does not prevent the compression station to fail from keeping the pressure level higher than the minimum set point value in case of sudden increase of gas withdrawal.

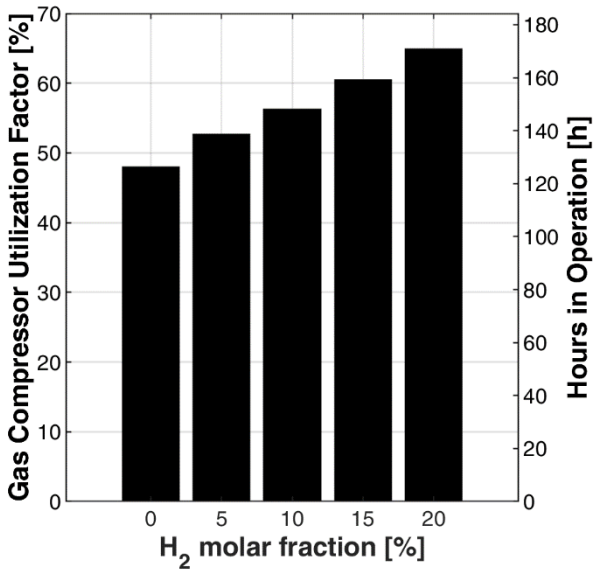

Figure 7 – Gas Compressor utilization factor and overall operating hours.

The bar plots of Figure 8 aim at giving aggregated values to summarize the variations in the behaviour of the gas compression station. Figure 8.a (left) depicts the overall mechanical energy released to the gas during the simulation timeframe and the corresponding overall gas consumption. It is worth noting that the overall compression work required in the case of 5% hydrogen is around 10% higher than the benchmark case while for the case of 10% hydrogen is 16%, 25% with 15% hydrogen blending, this increment grows to 32.5% with 20% hydrogen concentration. Figure 8.b (right) depicts instead the average values of the shaft power and of the gas consumption of the compressor, obtained by dividing the overall values of mechanical energy and gas consumption by the number of operating hours. In this case it is possible to note that the average shaft power required by the compressor slightly decreases as the hydrogen molar fraction increases (because of the increase of the compressor operating time and lower pressure at Gela terminal) while the average gas consumption rate increase as an effect of the lower volumetric heating value of the hydrogen-natural gas blends.

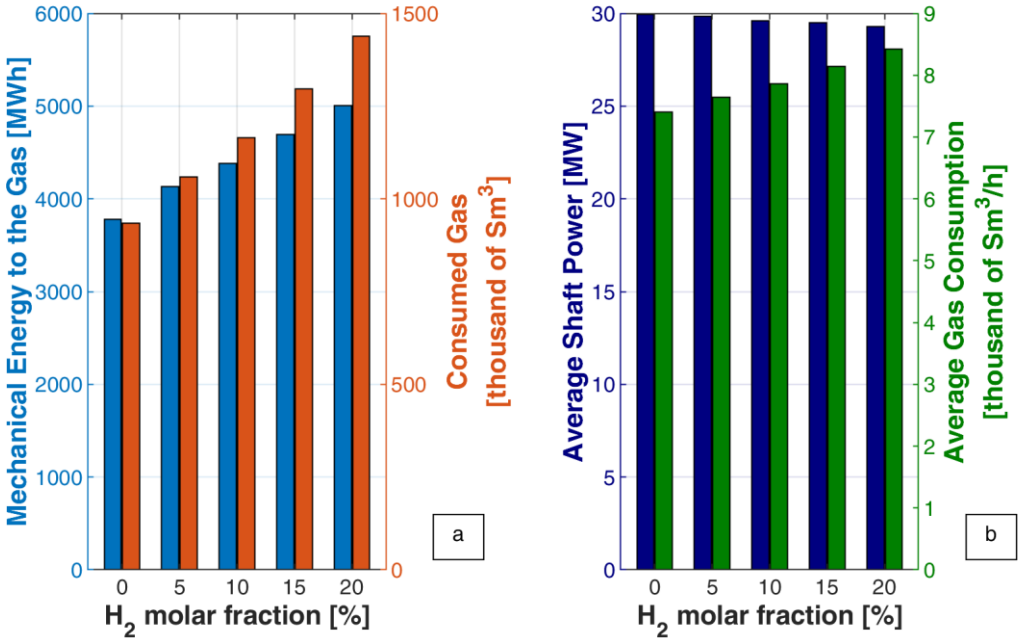

Figure 8 – a) overall mechanical energy provided to the gas for its compression and corresponding overall consumed gas for the five hydrogen blending cases; b) average shaft power and average gas consumption rate for the five hydrogen blending cases.

In relative value, compression work accounts for around 0.5% of total energy transported by the transmission infrastructure that increases at 0.7% when 20% hydrogen blend is transported.

5.2 Sizing of the solar hydrogen production facilities.

A further objective of the simulation of the portion of the Western Libyan infrastructure is to determine the patterns of admissible hydrogen at the injection points. The aim is to evaluate the renewables storage potential of the infrastructure under real case working condition and to size possible future renewable hydrogen facilities whose production is to be matched to the gas network receiving capability.

According to the assumption made, the modelled gas network has been constrained on gas flows only at the outlet nodes of Gela and of the domestic gas market. Thus, the inlet gas flows at Wafa field and at the Mellitah Gas Processing plant are the results of the interplay between gas withdrawals, gas station operation and the fluid-dynamic of the pipelines. Having assumed that the hydrogen is blended at the two injection points so to guarantee a fixed and constant molar fraction, the pattern of hydrogen injected for the two nodes is the one depicted in Figure .

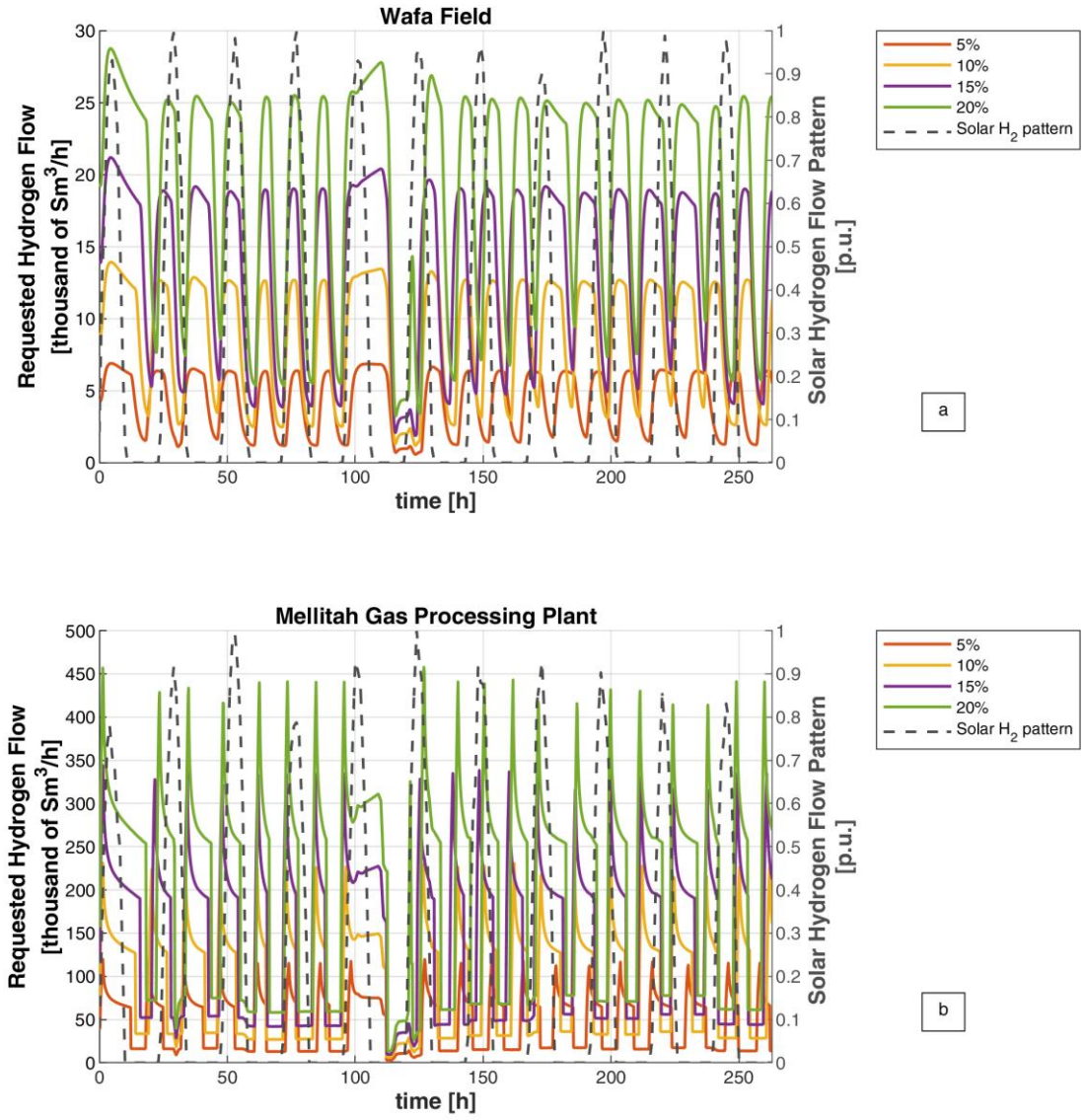

Figure 9 – Hydrogen injection pattern at the inlet nodes of the modeled gas infrastructure for the four injection scenarios superimposed to the nominal possible hydrogen pattern generated from electricity from a dedicated photovoltaic plant (in p.u. , referred to the right axis). Figure a refers to the Wafa Field area; figure b to the Mellitah Gas Processing Plant

As it is possible to see, not only the magnitude of the maximum injectable hydrogen, but also the injection pattern is significantly different between the two locations. It is interesting to note that, for both the locations, the cycling pattern is related to the compression station operating mode, with the hydrogen injection profile at the Mellitah Gas Processing Plant being closely linked to the compressor operating status. This is caused by the proximity of this injection point to the compression station. In Figure 9 a and b the possible hydrogen pattern generated from an electrolyzer exclusively powered by a photovoltaic plant is also superimposed. It is expressed in “per unit” i.e. as a fraction of the maximum production rate within the considered timeframe, so to give emphasis to the profile. As it is possible to note, the frequency of the oscillations of the hydrogen

acceptability by the gas network is higher than the one of the solar hydrogen production, leading to mismatches between hydrogen production and the gas network receiving capacity. What is more, the hydrogen production from photovoltaic drops to zero during the night time while the receiving capacity of the gas pipelines never goes to zero as the gas flow never stops along the main transmission infrastructure (unless critical events happen).

The mismatch between the hydrogen production and the pipeline receiving capacity and the discontinuous production from solar source call for the need of a suitable storage system if a constant share of hydrogen over time is to be guaranteed. The size of photovoltaic field that is dedicated to power the electrolyzers depends on the size of the related hydrogen storage.

As for the electrolyzers, the hydrogen conversion efficiency was assumed to be equal to $65\%_{HHV}$, that is an average value within the common range of alkaline and proton-exchange-memebrane (PEM) type [58],[59]. Alkaline and PEM electrolyzers are also the most suitable technology for a coupling with variable renewable energy sources according to the abundant literature [60],[61] and the several projects on these systems [62],[63]. Their nominal power will follow the actual solar power production, so to be able to convert completely the renewable power to a hydrogen flow without the need of any battery pack for electricity storage. Since the pressure level of the natural gas pipeline ranges between $75 \div 80$ bar_g, the hydrogen needs to be compressed up to the required pressure for injection or storage. The most suitable electrolyzers able to provide hydrogen at higher pressure are PEM ones, reaching pressures up to 30 bar_g [64]. A further compression stage is, in general, required. A possible option for hydrogen storage may be given by pipes storage [9],[65][66]

For both locations, the photovoltaic hourly plant production has been obtained using the PV-GIS web tool by JRC [67]. A fixed axis, crystalline silicon, 1 MW_p photovoltaic plant with 14% of system losses has been considered for the tilt and azimuth angles optimization evaluating the overall production over the full PV-GIS weather database (2005-2016). The main technical specifications for both the locations are summarized in Table 5.

Table 5 – Technical specification of the photovoltaic unit plants as obtained from the optimization tool by PV-GIS [67].

Location	Nominal Power [p.u.]	Installation type	Module type	System losses [%]	Tilt angle [°]	Azimuth angle [°]
Wafa	1	Fixed	Crystalline Silicon	14	30	0
Mellitah Gas Processing Plant	1	Fixed	Crystalline Silicon	14	31	4

The hourly plant production for the period 2005-2016 has been obtained from the PV- GIS tool and it has been used to generate a typical solar production year by averaging the hourly solar production over the whole period. The optimal sizing of the two photovoltaic plants has been based on the averaged values and restricted to the 11-day timeframe for which the gas network simulations have been obtained. The objective function consisted in the amount of hydrogen that needs to be stored in order to compensate the mismatch between the

production and the pipeline receiving capacity. The size of the storage depends on the nominal installed power of photovoltaic. The optimization procedure aims at determine the solar plant size which minimizes the storage volume needed within the 11-day timeframe considered before. Figure 10 and Figure 11 give the main results of this procedure for the four hydrogen blending cases and for the two locations considered (Wafa field and the Mellitah Gas Processing Plant respectively). In both figures, the mismatch between the hydrogen production and the hydrogen receiving capacity is given in terms of hydrogen chemical power with positive values indicating an overproduction of hydrogen. The temporal profile of the amount of hydrogen stored within the storage facility is given accordingly depicting the status of the storage that is varied in order to keep the hydrogen share of the blend constant. The maximum value of each curve represents the storage required for each case and it is reported for the sake of comparison in the middle bar plot at the side.

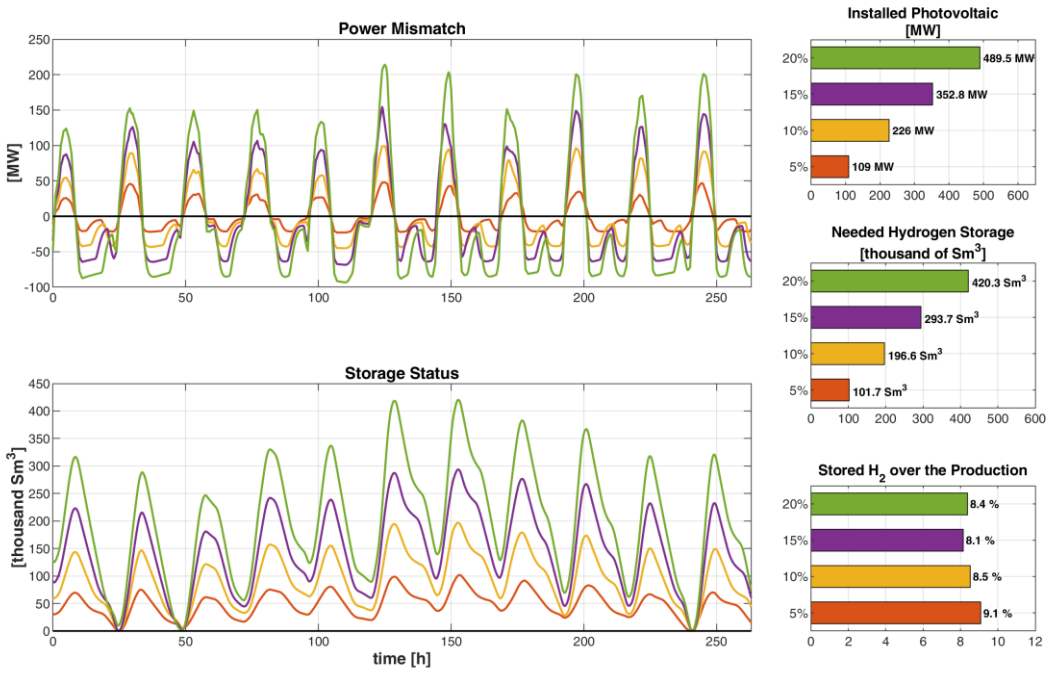

Figure 10 – Results of the Wafa photovoltaic plant optimal sizing procedure consisting in the minimization of the hydrogen storage needs. The two line graphs represents (top) the hydrogen production-injection mismatch (in chemical power terms) and (bottom) the temporal profile of the amount of hydrogen stored within the storage system. The side bar plots indicates (from top to the bottom): the optimal photovoltaic plant size, the amount of hydrogen that needs to be stored and the percentage of the size of the hydrogen storage over the overall hydrogen production within the considered timeframe of 11 days.

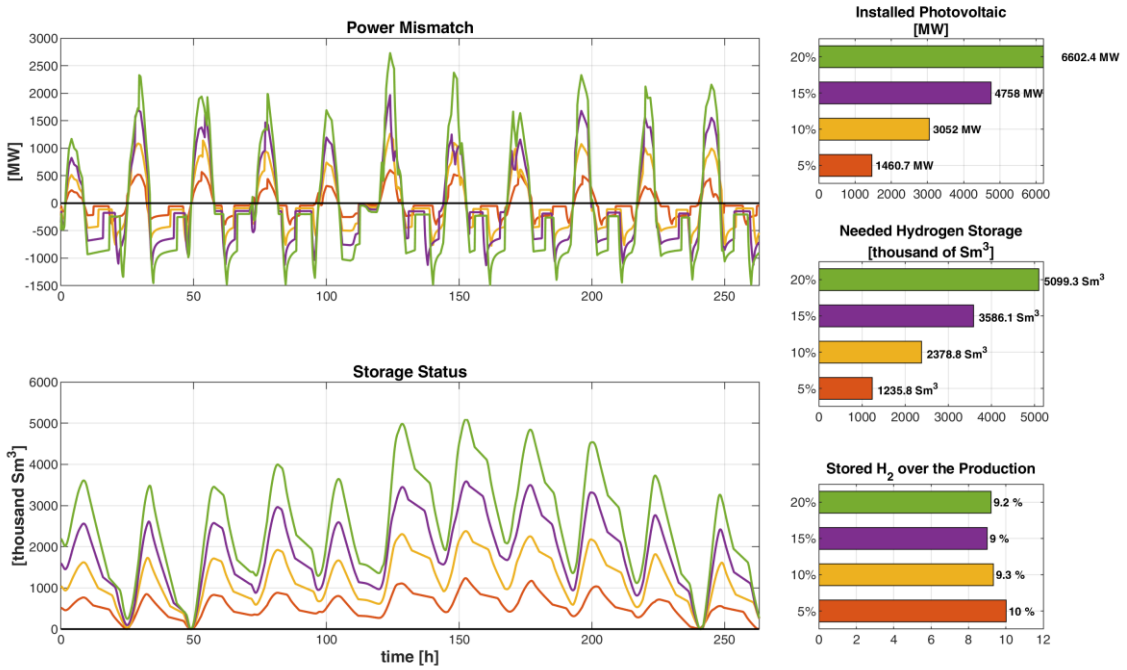

Figure 11 – Results of the Mellitah photovoltaic plant optimal sizing procedure consisting in the minimization of the hydrogen storage needs. The two line graphs represents (top) the hydrogen production-injection mismatch (in chemical power terms) and (bottom) the temporal profile of the amount of hydrogen stored within the storage system. The side bar plots indicates (from top to the bottom): the optimal photovoltaic plant size, the amount of hydrogen that needs to be stored and the percentage of the size of the hydrogen storage over the overall hydrogen production within the considered timeframe of 11 days.

The value of the storage, for each of the four blending cases, is the result of the storage minimization procedure described before that carried to the determination of the optimal power of the photovoltaic plants. For what concerns the Wafa case, the sizes range from 109 MW to 489.5 MW as the hydrogen blending target grows from 5 to 20% (upper bar plot of Figure 10) while for the Mellitah location, the sizes exceed the gigawatt scale, ranging from 1.5 GW to 6.6 GW (upper bar plot of Figure 1).

As a final indicator, the ratio between the size of the required hydrogen storage over the total hydrogen produced within the considered 11 days is given in percentage terms in the lower bar plot of the figures, in order to indicate the importance of the storage on the production. For Wafa site it ranges between 8.1 and 9.1% while for the Mellitah one these values are slightly higher, ranging between 9 and 10 %. These numbers give a measure of the minimum storage size required to overcome the mismatches between solar energy availability and the pipeline flow management.

Concerning the electrolyzers, following the sizing assumption aforementioned that aimed at avoiding any electrical storage devices, the results of the sizing process are given in

Table 6.

Table 6 – Electrolyzers rated power

Location		Cases			
		5 %	10 %	15 %	20 %
Wafa	[MW]	81.0	167.9	262.1	363.6
Mellitah Gas Processing Plant	[MW]	968.1	2022.7	3153.3	4375.7

6 Discussion

The fluid dynamic modelling of the portion of the Libyan gas infrastructure shows a non-negligible impact of the hydrogen blending already in the range [0% – 20%]. The increase of volume caused by the decrease of the volumetric higher heating value as the hydrogen fraction grows causes an increase of the work of compression up to 32.5% during the time interval addressed by the simulation. What is more, the results of the fluid-dynamic simulations show that the usual control strategy of the compression station adopted for the 100% natural gas case is not suitable anymore already if the 5% of hydrogen is blended within the natural gas. In fact, the contractual constraint on the pressure at Gela Station is not respected anymore. This aspect, together with the potentially detrimental effect that the hydrogen-natural gas blends may have on the combustion efficiency at the turbo-compressor (that has not been considered in this work), may amplify the overall increasing operational costs. However, the increase of the compressor station consumption has a very little impact on the efficiency of the gas transport system: by losing less than 0.2 % point of transport efficiency (at maximum), the gas transport network is able to provide an energy flux that is up to 7% from renewables.

As for the gas quality parameters, the impact of the hydrogen blending on the relative density, on the higher heating value and on the Wobbe Index of the gas can be evaluated with respect to the composition of the Libya natural gas and compared with the upper and lower limits of each parameter as set by the Italian national regulation [68]. It is interesting to note that, in the case of Libyan natural gas the hydrogen acceptability is up to 15% and the limiting parameter is the Wobbe Index[1]. It is important to underline that these quality indicators are not exhaustive nor comprehensive in order to decree the acceptability of the hydrogen blending. However, these are the most widely used among the TSOs in order to monitor the acceptability of natural gas from different origins. What is more, most of the gas network value chain is ready to accept up to 15 – 20 % of hydrogen according to [23].

[1] The Wobbe Index is defined as the ratio between the fuel gas heating value (higher or lower) and the square root of its relative density

$$WI = HHV/\sqrt{RD}$$

Where the relative density of a gas is the ratio of the density of the gas to the density of the air both calculated at standard pressure and temperature conditions.
In this work: normal conditions [$T_n = 273.15\ K$, $p_n = 101{,}325\ Pa$];
Standard conditions [$T_{STD} = 288.15\ K$, $p_{STD} = 101{,}325\ Pa$];

A superposition of the solar hydrogen production duration curves resulting from the optimal sizing process with the duration curves of the hydrogen receiving potential are given in Figure 12 for both the considered locations. The solid curves represent the hydrogen production from solar source while the dashed lines represent the pipeline receiving capacity. The role of the storage is fundamental in order to store the overproduction to be shifted whenever the solar source is missing or non-sufficient (from about time, 120 h in the figures).

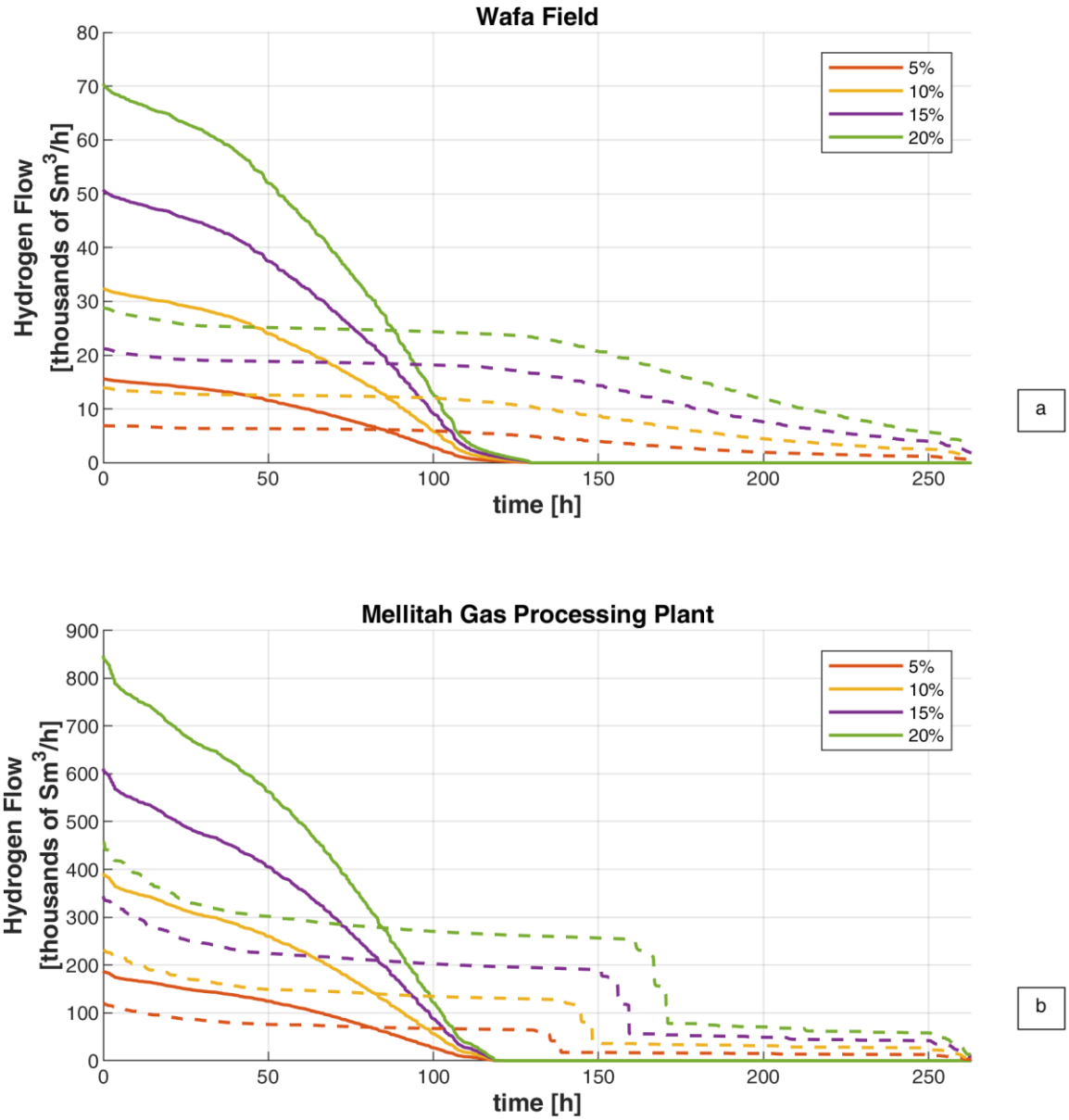

Figure 12 – Duration curves of the hydrogen production from solar source (solid lines) and hydrogen acceptability within the natural gas stream (dashed lines).

According to the assumption made this duration curves represent also the output of the electrolyzers and show a low capacity factor operation of 26.8% for the Wafa case and of 23.9% for the Mellitah installation. Indeed, the electrolyzers only operate for about 120 h and modulate over their full operational range.

7 Conclusions

In this work, the impact of the practice of hydrogen blending within one of the European gas import stream form North Africa, the Greenstream, was assessed by means of the application of a gas network fluid-dynamic model.

The goal was first to evaluate the additional costs in terms of energy consumption at compressor stations. Four blending scenarios have been considered, with hydrogen share constantly fixed at 5%, 10%, 15% and 20%. It has been assumed that the hydrogen would have substituted a share of natural gas thus realizing a H_2-NG mixture with the same energy content as in the base case, without any hydrogen blending. This resulted in a higher overall volume of gas transported, as the volume-based higher heating value of the hydrogen is lower than the one of the natural gas.

The simulation was conducted without varying the assumed control mode of the gas compression station, which was preliminary verified to be suitable for the infrastructure requirements under no hydrogen scenario. It has been observed that already at 5% blends, the pressure level at the end of the infrastructure fails at reaching the minimum requested value under a peculiar moment of the simulation. As for the additional compression costs, the presence of hydrogen increases the number of hours of activity of the compressor and the overall gas consumption increases accordingly. However, in terms of transport efficiency, the amount of energy that is transported through pipeline is so high that the increment of the gas compression costs (which may be as high as 32.5%) impacts in a negligible way (an incremental increase of 0.2%) on the transport efficiency.

As final outcome of this work, a sizing procedure for a hydrogen production dedicated photovoltaic plant have been proposed, based on the minimization of the hydrogen storage. The results show that a considerable amount of hydrogen needs to be stored because of the pipeline availability is not always in phase with the hydrogen production profiles, even at lower hydrogen blends. It is also to be underlined that the case study under consideration consists in an intercontinental gas import pipeline thus even at lower share of hydrogen, the renewable power which is required is very high. In this sense, these case studies may help framing the 2x40 GW initiative form EU [31].

The key messages that this work aim to provide are the following:

1) The amount of renewable that can be conveyed through hydrogen blending is considerable (considering the high capacity transnational pipeline) and it is available at rather low additional operational costs in terms of energy;
2) However, the pipeline availability in accepting hydrogen may not be infinite. Requiring a constant share of hydrogen within the natural gas blend limits the flexibility of the natural gas system thus imposing some barriers to the opportunities offered by the system integration.

In this case, the hydrogen storage needs have emerged as potential barriers.

Future works may be headed to the opportunities offered by some variations in the gas compressor management system so to increase the hydrogen acceptability within the gas infrastructure or to reduce mismatches by phasing gas fluxes to the hydrogen production profiles. In a broader context, the choice of the type of storage (either electrochemical or in gaseous form or both) and its optimal sizing, together with innovative infrastructure management strategies, should also be addressed in order to evaluate the realistic added-value of sectorial integration through green hydrogen from power-to-gas.

References

[1] European Parliament. Regulation (EU) 2018/1999 of the European Parliament and of the Council of 11 December 2018 on the Governance of the Energy Union and Climate Action. vol. 328. 2018. https://doi.org/https://eur-lex.europa.eu/legal-content/EN/TXT/PDF/?uri=CELEX:32018R1999&from=EN.

[2] European Commission. The European Green Deal - COM(2019) 640. Brussels: 2019.

[3] European Commission. Europe's moment: Repair and Prepare for the Next Generation - COM(2020) 456. Brussels: 2020. https://doi.org/10.1017/CBO9781107415324.004.

[4] European Commission. An EU Strategy for Energy System Integration- COM(2020) 299. COM(2020) 299 2020.

[5] European Commission. A hydrogen strategy for a climate-neutral Europe - COM(2020) 301. COM(2020) 301 2020.

[6] Staffell I, Scamman D, Velazquez Abad A, Balcombe P, Dodds PE, Ekins P, et al. The role of hydrogen and fuel cells in the global energy system. Energy Environ Sci 2019;12:463–91. https://doi.org/10.1039/c8ee01157e.

[7] IEA. The Future of Hydrogen. Seizing today's opportunities. 2019.

[8] Speirs J, Balcombe P, Johnson E, Martin J, Brandon N, Hawkes A. A greener gas grid: what are the options? 2017.

[9] Andersson J, Grönkvist S. Large-scale storage of hydrogen. Int J Hydrogen Energy 2019;44:11901–19. https://doi.org/10.1016/j.ijhydene.2019.03.063.

[10] Rahman MM, Oni AO, Gemechu E, Kumar A. Assessment of energy storage technologies: A review. Energy Convers Manag 2020;223:113295. https://doi.org/10.1016/j.enconman.2020.113295.

[11] Snam, International Gas Union, The Boston Consulting Group. Global gas report 2018. 2018.

[12] Snam, Union IG, BloombergNEF. Global Gas Report 2020. 2020.

[13] Pöyry. Fully decarbonising Europe's energy system by 2050 Decarbonising Europe's energy system. 2018.

[14] Ecofys. Gas for Climate: How gas can help to achieve the Paris Agreement target in an affordable way. 2018.

[15] You C, Kim J. Optimal design and global sensitivity analysis of a 100% renewable energy sources based smart energy network for electrified and hydrogen cities. Energy Convers Manag 2020;223:113252. https://doi.org/10.1016/j.enconman.2020.113252.

[16] McKinsey Energy Insights. Global Energy Perspective 2019 : Reference Case. 2019.

[17] IRENA. Global Energy Transformation - A Roadmap to 2050.pdf. 2019.

[18] IRENA. Global Renewables Outlook: Energy transformation 2050. 2020.

[19] IEA. World Energy Outlook 2019. 2019.

[20] Navigant. Gas for Climate. The optimal role for gas in a net-zero emissions energy system. Navig Netherlands BV 2019:231.

[21] Melaina MW, Antonia O, Penev M. Blending Hydrogen into Natural Gas Pipeline Networks: A Review of Key Issue. 2013.

[22] Altfeld K, Pinchbeck D. Admissible hydrogen concentrations in natural gas systems. 2013.

[23] Marcogaz. Overview of Available Test Results and Regulatory Limits for Hydrogen Admission into Existing Natural Gas Infrastructure and End Use. 2019.

[24] American Petroleum Institute (API). API Standard 617 - Axial and Centrifugal Compressors and Expander-compressors 2014.

[25] Abbott DJ, Bowers JP, James SR. The Impact of Natural Gas Composition Variations on the

Operation of Gas Turbines for Power Generation. Futur. Gas Turbine Technol. 6th Int. Conf., Brussels, Belgium: 2012, p. 1.

[26] de Vries H, Mokhov A V., Levinsky HB. The impact of natural gas/hydrogen mixtures on the performance of end-use equipment: Interchangeability analysis for domestic appliances. Appl Energy 2017;208:1007–19. https://doi.org/10.1016/J.APENERGY.2017.09.049.

[27] Larfeldt J, Anderson M, Larsson A, Moell D. Hydrogen Co-Firing in Siemens Low NO X Industrial Gas Turbines. Power-Gen Eur., Cologne, Germany: 2017.

[28] Snam, Hughes B. Snam and Baker Hughes test world's first hydrogen blend turbine for gas networks 2020.

[29] Directorate-General For Energy and Transport. Mandate to CEN for standardisation in the field of gas qualities 2007.

[30] UNI/EN. UNI 16726:2018 2018.

[31] Wijk A van, Chatzimarkakis J. Green Hydrogen for a European Green Deal - A 2x40 GW Initiative. 2020.

[32] Enagás, Energinet, Fluxys Belgium, Gasunie, GRTgaz, NET4GAS, et al. European Hydrogen Backbone. 2020.

[33] Wijk A van, Wouters F, Rachidi S, Ikken B. A North Africa-Europe Hydrogen Manifesto. Dubai, London, Madrid,Munich: 2020.

[34] Timmerberg S, Kaltschmitt M. Hydrogen from renewables: Supply from North Africa to Central Europe as blend in existing pipelines – Potentials and costs. Appl Energy 2019;237:795–809. https://doi.org/10.1016/j.apenergy.2019.01.030.

[35] Pellegrino S, Lanzini A, Leone P. Greening the gas network: the need for modelling the multi-dimensional injection of alternative fuels. Renew Sustain Energy Rev 2017;70:266–286.

[36] Guandalini G, Colbertaldo P, Campanari S. Dynamic modeling of natural gas quality within transport pipelines in presence of hydrogen injections. Appl Energy 2017;185:1712–23.

https://doi.org/10.1016/J.APENERGY.2016.03.006.

[37] Chaczykowski M, Zarodkiewicz P. Simulation of natural gas quality distribution for pipeline systems. Energy 2017;134:681–98. https://doi.org/10.1016/j.energy.2017.06.020.

[38] Fragiacomo P, Genovese M. Technical-economic analysis of a hydrogen production facility for power-to-gas and hydrogen mobility under different renewable sources in Southern Italy. Energy Convers Manag 2020;223:113332. https://doi.org/10.1016/j.enconman.2020.113332.

[39] Pambour KA, Bolado-Lavin R, Dijkema GPJ. An integrated transient model for simulating the operation of natural gas transport systems. J Nat Gas Sci Eng 2016;28:672–90. https://doi.org/10.1016/j.jngse.2015.11.036.

[40] Kunz O, Wagner W. The GERG-2008 wide-range equation of state for natural gases and other mixtures: An expansion of GERG-2004. J Chem Eng Data 2012;57:3032–91. https://doi.org/10.1021/je300655b.

[41] Shashi Menon E. Gas Pipeline Hydraulics. Taylor & Francis; 2005.

[42] Kiuchi T. An implicit method for transient gas flows in pipe networks. Int J Heat Fluid Flow 1994;15:378–83.

[43] Abbaspour A, Chapman KS. Nonisothermal Transient Flow in Natural Gas Pipeline. J Appl Mech 2008;75:1–8. https://doi.org/10.1115/1.2840046.

[44] van der Hoeven T. Math in Gas and the art of linearization. University of Groningen, 2004.

[45] Cerbe G. Grundlagen der Gastechnik. München: Hanser; 2008.

[46] Eurostat. Natural Gas Supply Statistics. Eurostat - Stat Explain 2019.

[47] Eni N. greenstreambv.com n.d.

[48] Italian Ministry of Economic Development. Decreto direttoriale 31 gennaio 2017 - Aggiornamento della Rete Nazionale dei Gasdotti 2017.

[49] NOC. National Oil Corporation website n.d.

[50] ETN Global. Gas Turbine Products/MS5002D n.d.

[51] Mellitah Oil and Gas Co. Wafa Field Gas Compressor Project Press Release 2018.

[52] Eni.com. Bahr Essalam Phase 2 Development offshore project begins production 2018.

[53] Snam. Snam - Portale Misura. MisuraSnamIt n.d.

[54] ENTSOG. ENTSOG Transparency Platform n.d.

[55] Ciprigno M, Ftis A, Agostoni A. Greenstream Project Gas Export System From Libya To Italy. Offshore Mediterr. Conf. Exhib., Ravenna, Italy: Offshore Mediterranean Conference; 2005, p. 10.

[56] Dossier Sicilia - Gas. Quarr Constr 2005:166–7.

[57] Snam Rete Gas. Piano decennale di sviluppo della rete di trasporto del gas naturale 2020-2029. 2020.

[58] Ferrero D, Gamba M, Lanzini A, Santarelli M. Power-to-Gas Hydrogen: Techno-economic Assessment of Processes towards a Multi-purpose Energy Carrier. Energy Procedia 2016;101:50–7. https://doi.org/10.1016/j.egypro.2016.11.007.

[59] Holladay JD, Hu J, King DL, Wang Y. An overview of hydrogen production technologies. Catal Today 2009;139:244–60. https://doi.org/10.1016/j.cattod.2008.08.039.

[60] Mazza A, Bompard E, Chicco G. Applications of power to gas technologies in emerging electrical systems. Renew Sustain Energy Rev 2018;92:794–806. https://doi.org/10.1016/j.rser.2018.04.072.

[61] Sterner M. Bioenergy and renewable power methane in integrated 100% renewable energy systems. kassel university, 2009.

[62] Gahleitner G. Hydrogen from renewable electricity: An international review of power-to-gas pilot plants for stationary applications. Int J Hydrogen Energy 2013;38:2039–61. https://doi.org/10.1016/j.ijhydene.2012.12.010.

[63] Horizon 2020 project. Store&Go n.d.

[64] Tractebel-Engie, Hincio. Study on Early Business Cases for H2 in Energy Storage and More Broadly Power To H2 Applications. 2017.

[65] Kruck O, Crotogino F, Prelicz R, Rudolph T. HyUnder Deliverable - Overview on all Known

Underground Storage Technologies for Hydrogen. 2013.

[66] Marcogaz, eurogas, GERG. Gas Bridges : the natural gas network as key partner of the energy transition. 2017.

[67] JRC. PV-GIS n.d.

[68] Italian Ministry of the Interior. D.M. 18/05/2018 - Regola tecnica sulle caratteristiche chimico fisiche e sulla presenza di altri componenti nel gas combustibile 2018.